Copy
RM L52B15a

RESEARCH MEMORANDUM

AN INVESTIGATION OF LONGITUDINAL CONTROL CHARACTERISTICS OF A WING-TIP CONTROL SURFACE ON A SWEPTBACK WING AT TRANSONIC SPEEDS BY THE NACA WING-FLOW METHOD

By James P. Trant, Jr.

Langley Aeronautical Laboratory
Langley Field, Va.

NATIONAL ADVISORY COMMITTEE
FOR AERONAUTICS

WASHINGTON
June 13, 1952

NATIONAL ADVISORY COMMITTEE FOR AERONAUTICS

RESEARCH MEMORANDUM

AN INVESTIGATION OF LONGITUDINAL CONTROL CHARACTERISTICS OF A WING-TIP CONTROL SURFACE ON A SWEPTBACK WING AT TRANSONIC SPEEDS BY THE NACA WING-FLOW METHOD

By James P. Trant, Jr.

SUMMARY

An investigation of the longitudinal control effectivness of a full-chord wing-tip control surface on a wing having 35° sweepback, 12 percent thickness perpendicular to the quarter-chord line, an aspect ratio of 3.01, and a taper ratio of 0.605 was made by the NACA wing-flow method at Mach numbers ranging from 0.65 to 1.1. The results showed that the wing-tip control was only 1/6 as effective in producing pitching moment at subsonic speeds as a flap-type control on a model with the same wing and was 1/2 as effective at low-supersonic speeds. The wing-tip control became ineffective with some tendency toward reversal in the Mach number range from 0.9 to 1.0.

In general, the hinge-moment coefficient had large irregular variations with angle of attack, control deflection, and Mach number, particularly at Mach numbers from 0.9 to 1.0.

INTRODUCTION

Results of unpublished tests to determine the longitudinal control effectiveness of a trailing-edge flap-type control surface on a 35° sweptback wing of a tailless airplane model indicated large losses in and, in some conditions, reversal of control effectiveness at transonic speeds. The present investigation was made to determine whether the loss of longitudinal control effectiveness would be avoided by use of full-chord wing-tip control surfaces of approximately the same area as the flap-type controls on a wing of the same dimensions. Other tests of wing-tip controls on sweptback wings (refs. 1 to 3) have indicated nearly constant effectiveness characteristics at transonic speeds. Since there appears to be little available information on

hinge-moment characteristics of wing-tip controls on sweptback wings at transonic speeds, the present investigation also included tests to determine hinge-moment characteristics. Tests were made at three control deflections without an end plate and for one deflection with an end plate between the wing-tip control and the wing. Measurements were made of normal force, pitching moment, hinge moment, and angle of attack over a Mach number range of about 0.65 to 1.1. The corresponding average Reynolds numbers varied from 1.32×10^6 to 1.86×10^6.

SYMBOLS

S	wing area of model
S_t	area of control surface
c	local chord of model
$\bar{c}$	mean aerodynamic chord of model
$\bar{c}_t$	mean aerodynamic chord of control surface
R	Reynolds number (based on $\bar{c}$)
M	effective Mach number
q	effective dynamic pressure
α	angle of attack
δ	control deflection (measured in a plane normal to the Y-axis)
C_N	normal-force coefficient (Normal force/qS)
C_m	pitching-moment coefficient about 17-percent-$\bar{c}$ point (Pitching moment/$qS\bar{c}$)
C_h	hinge-moment coefficient about 25-percent-$\bar{c}_t$ point (Hinge moment/$qS_t\bar{c}_t$)
$\partial C_m/\partial C_N$	pitching-moment-curve slope
$\partial C_N/\partial \alpha$	normal-force-curve slope

APPARATUS AND TESTS

The model was tested at transonic speeds by the NACA wing-flow method in which the semispan model is mounted in the high-speed flow over the wing of an F-51D airplane, the wing serving as a reflection plane for the model. The method is similar to that described in more detail in reference 4.

Figure 1 is a photograph of the semispan model mounted on the wing of the airplane. The details of the model are shown in photographs, figures 2 and 3, and a drawing, figure 4. The model had symmetrical airfoil sections 12 percent thick perpendicular to the 35° sweptback quarter-chord line. Ordinates for the airfoil sections parallel to the plane of symmetry are given in table I. The model had a taper ratio of 0.605 and an aspect ratio of 3.01 (the F-51D wing being considered as a reflection plane).

The full-chord wing-tip control surface consisted of the portion of the wing extending outboard of the 84.8-percent-semispan station. The gap between the inboard portion of the model and the tip control for a control deflection of -0.5° was 0.016 inch at the leading edge and 0.035 inch at the trailing edge. The control was mounted on a shaft extending along the quarter-chord line of the model. Control-surface hinge moments were measured by means of a strain-gage balance attached to this shaft.

Normal force and pitching moment on the entire model were measured by means of a strain-gage balance located within the wing of the F-51D airplane and attached to the shank of the model. The hole in the airplane wing surface through which the model shank and the control shaft extended was covered by a root-chord-diameter circular end plate attached to the model. The model and the balance for measuring normal force and pitching moment were arranged to rotate as a unit through -1° to 11° angle of attack at a rate of about 1/2 cycle per second. The center of rotation of the model and the center line of the balance were at 35 percent of the mean aerodynamic chord. The angle of the model with reference to a line on the wing of the F-51D airplane was measured by a slide-wire potentiometer. A free-floating vane, shown in figure 1, was used to determine the direction of air flow at the model location. The angle of attack was determined from the angles measured with the potentiometer and the vane.

The chordwise and vertical gradients of velocity over the F-51D airplane wing in the region of the model were similar to those of the tests of reference 4. The effective Mach number M and the effective dynamic pressure q were determined by integrating their distributions over the area covered by the model wing.

[redacted]

Tests were made with the control surface deflected -0.5°, -12.2°, and -17.2°. These deflections were measured in a plane perpendicular to the Y-axis of the model. One test at the -17.2° deflection was made with an elliptical end plate attached to the root chord of the tip control (fig. 3). The major axis of the end plate was equal in length to the root chord of the tip control and the minor axis was equal to one-half the major axis.

The tests were made by diving the airplane to a medium altitude and continuing the dive within the placard limits of the airplane to a low altitude where a pull-out and deceleration to low speed were effected. This maneuver gave the maximum Reynolds number at a given Mach number attainable within the placard limits of the airplane. The average relation between Mach number and Reynolds number is shown in figure 5.

The accuracy of the results is indicated in figure 6 which shows the typical scatter in angle of attack, pitching-moment coefficient, and hinge-moment coefficient for zero normal-force coefficient and -0.5° control deflection as obtained by the wing-flow method in this investigation. The control deflections given are accurate to ±0.3° since the wing-tip control twists this amount for the maximum hinge moment exerted on it. No correction for this twist was applied to the control deflection in this investigation.

PRESENTATION OF RESULTS

The results of the tests are presented in figures 7 to 15. The variations of angle of attack and pitching-moment coefficient with Mach number for several normal-force coefficients are shown in figures 7 and 8, respectively, for the test with control near neutral (δ = -0.5°). The variations with Mach number in the rate of change of normal-force coefficient with angle of attack and in the rate of change of pitching-moment coefficient with normal-force coefficient are shown in figure 9 for a hypothetical airplane with -0.5° control deflection at the trim normal-force coefficient for level flight at 30,000 feet with a wing loading of 28 pounds per square foot. The variation of pitching-moment coefficient with normal-force coefficient for three control deflections (-0.5°, -12.2°, and -17.2°) without the tip-control end plate and one deflection (-17.2°) with the tip-control end plate at several Mach numbers is shown in figure 10. The variation of pitching-moment coefficient with control deflection is shown in figure 11 for two angles of attack and in figure 12 for C_N = 0.1 at various Mach numbers. Figure 12 also contains results from the tests of the fin-off flap-type configuration for comparison purposes. The variations of hinge-moment

coefficient with Mach number for several normal-force coefficients are shown in figure 13 for the test with the control near neutral ($\delta = -0.5°$). Figure 14 is a presentation of the hinge-moment-coefficient variation with angle of attack for the three control deflections without the tip-control end plate and one deflection with the tip-control end plate at several Mach numbers and figure 15 shows the variation of hinge-moment coefficient with control deflection for two angles of attack at several Mach numbers.

It should be noted that the points identified by symbols in figures 11 and 12 are taken from the faired curves of figure 10 and normal-force curves faired from figure 7 and similar curves for the higher deflections. Also, the points identified by symbols in figure 15 are taken from the faired data of figure 14.

DISCUSSION

The results given in figure 7 indicate in general only moderate variations of angle of attack at constant normal-force coefficients over the Mach number range. The slope $\partial C_N/\partial \alpha$ of the normal-force curve in figure 9 was somewhat greater than 0.06 except at Mach numbers between about 0.9 and 1.0. At Mach numbers from 0.63 to 0.75 the static-longitudinal-stability margin $\partial C_m/\partial C_n$ (with the center of gravity at 17 percent M.A.C.) was 5 percent mean aerodynamic chord and increased to 12 percent at a Mach number of 0.9. With further increase in Mach number to 0.96 the margin decreased to a negative value of about 3 percent at a Mach number of 0.96 and then again reached a maximum of 20 percent at a Mach number of 1.05. The irregular variation of static margin between Mach numbers of 0.9 and 1.05 occurs mainly at normal-force coefficients below about 0.3. For normal-force coefficients higher than about 0.3 the variation in the static longitudinal stability margin with Mach number is more regular, as is shown in figures 8 and 10. The variations of pitching moment with control deflection (as can be seen in figs. 10, 11, and 12) show that the wing-tip control became ineffective with some tendency to reverse in the Mach number range from 0.9 to 1.0 and for normal-force coefficients near zero. For the same range of Mach number and normal-force coefficient, the unpublished results for the flap-type fin-off configuration of the tailless airplane model showed a large loss of control effectiveness and, in some conditions, reversal as is indicated in figure 12. The longitudinal control effectiveness of the wing-tip control as shown by the variation of C_m with control deflection in figures 10, 11, and 12 is approximately 1/6 of the longitudinal control effectiveness of the flap-type control at subsonic speeds. For Mach numbers greater than 1.0 the longitudinal control effectiveness of the wing-tip control was approximately the same as for the subsonic speeds but was approximately

one-half the effectiveness of the flap-type control at low-supersonic speeds. It should be noted that, in general, C_m for the wing-tip control was increasing at the maximum δ tested at all speeds and therefore the maximum C_m was not reached.

In general, the variations of hinge-moment coefficient with angle of attack were found to be large and irregular. Contrary to what might be expected for such a low-aspect-ratio plan form as the tip control, the change with Mach number of the variations of hinge moment with control deflection and with angle of attack was large as is indicated in figures 13, 14, and 15.

These large changes with Mach number and the irregular variations of C_h with deflection and angle of attack make it improbable that the hinge moments would be greatly reduced by selection of a different hinge axis. As a result, the forces on the control-actuating system calculated from the hinge-moment coefficients for a hypothetical full-scale airplane are so large as to be out of the range of booster control systems now practical.

An attempt was made to isolate the wing and the wing-tip-control pressure fields and to block any spanwise boundary-layer flow by use of an end plate separating the wing and wing-tip control surfaces as a possible means of reducing the hinge moments. Although no large beneficial effect was obtained from the addition of the end plate in reducing the hinge moments, a change in the pitching moment was effected at high values of C_N. Figure 10 shows that with the control deflected -17.2° at high values of C_N the addition of the end plate resulted in more positive C_m at a given C_N which indicates that the increased values of trim C_N could be obtained at all speeds except supersonic by use of the end plate.

CONCLUDING REMARKS

An investigation of the longitudinal control effectiveness of a full-chord wing-tip control surface on a wing having 35° sweepback, 12 percent thickness perpendicular to the quarter-chord line, an aspect ratio of 3.01, and a taper ratio of 0.605 was made by the NACA wing-flow method at Mach numbers ranging from 0.65 to 1.1. The results showed that the wing-tip control was only 1/6 as effective in producing pitching moment at subsonic speeds as a flap-type control on a model with the same wing and was 1/2 as effective at low-supersonic speeds. The wing-tip control became ineffective with some tendency toward reversal in the Mach number range from 0.9 to 1.0.

[redacted]

In general, the hinge-moment coefficient had large irregular variations with angle of attack, control deflection, and Mach number particularly at Mach numbers from 0.9 to 1.0.

Langley Aeronautical Laboratory
National Advisory Committee for Aeronautics
Langley Field, Va.

REFERENCES

1. Sandahl, Carl A., Strass, H. Kurt, and Piland, Robert O.: The Rolling Effectiveness of Wing-Tip Ailerons As Determined by Rocket-Powered Test Vehicles and Linear Supersonic Theory. NACA RM L50F21, 1950.

2. Stone, David G.: Comparisons of the Effectiveness and Hinge Moments of All-Movable Delta and Flap-Type Controls on Various Wings. NACA RM L51C22, 1951.

3. Moseley, William C., Jr., and Watson, James M.: Investigation of Wing-Tip Ailerons on a 51.3° Sweptback Wing at Transonic Speeds by the Transonic-Bump Method. NACA RM L51H27, 1951.

4. Johnson, Harold I.: Measurements of Aerodynamic Characteristics of a 35° Sweptback NACA 65-009 Airfoil Model with $\frac{1}{4}$-Chord Plain Flap by the NACA Wing-Flow Method. NACA RM L7F13, 1947.

[redacted]

TABLE I

ORDINATES OF AIRFOIL SECTION PARALLEL

TO CENTER LINE OF MODEL

Station (percent chord)	Ordinate (percent chord)
0	0
.6	1.1
.9	1.3
1.5	1.7
2.9	2.3
5.8	3.0
8.7	3.5
11.6	3.9
17.2	4.4
22.8	4.8
28.2	5.0
33.6	5.1
38.9	5.2
44.1	5.2
49.2	5.1
54.3	4.9
59.2	4.6
64.1	4.1
69.0	3.5
73.5	3.0
78.2	2.4
82.7	1.8
87.1	1.3
91.5	.9
95.8	.4
100.0	0

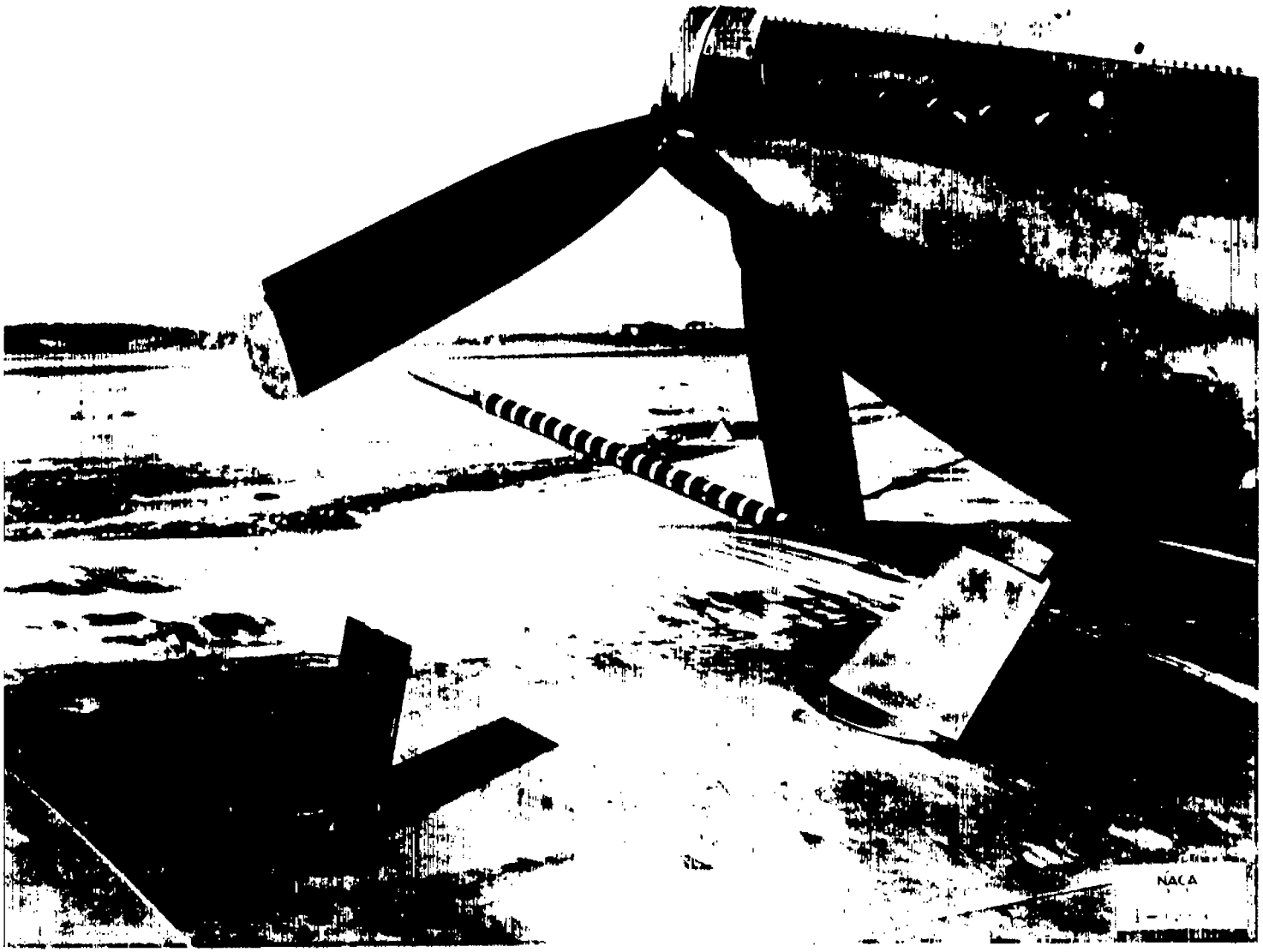

Figure 1.- Model and vane on wing of airplane.

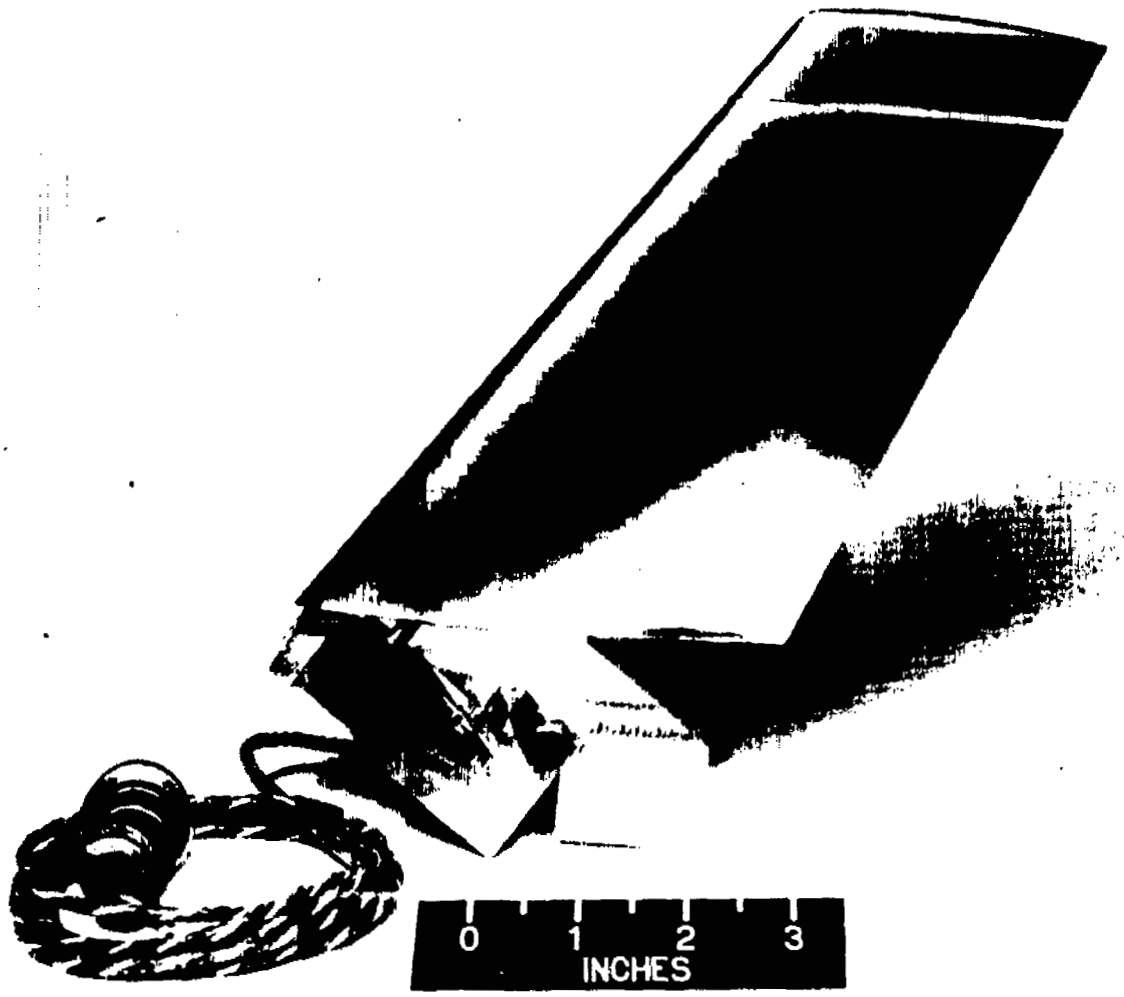

Figure 2.- Model (close-up showing hinge-moment balance).

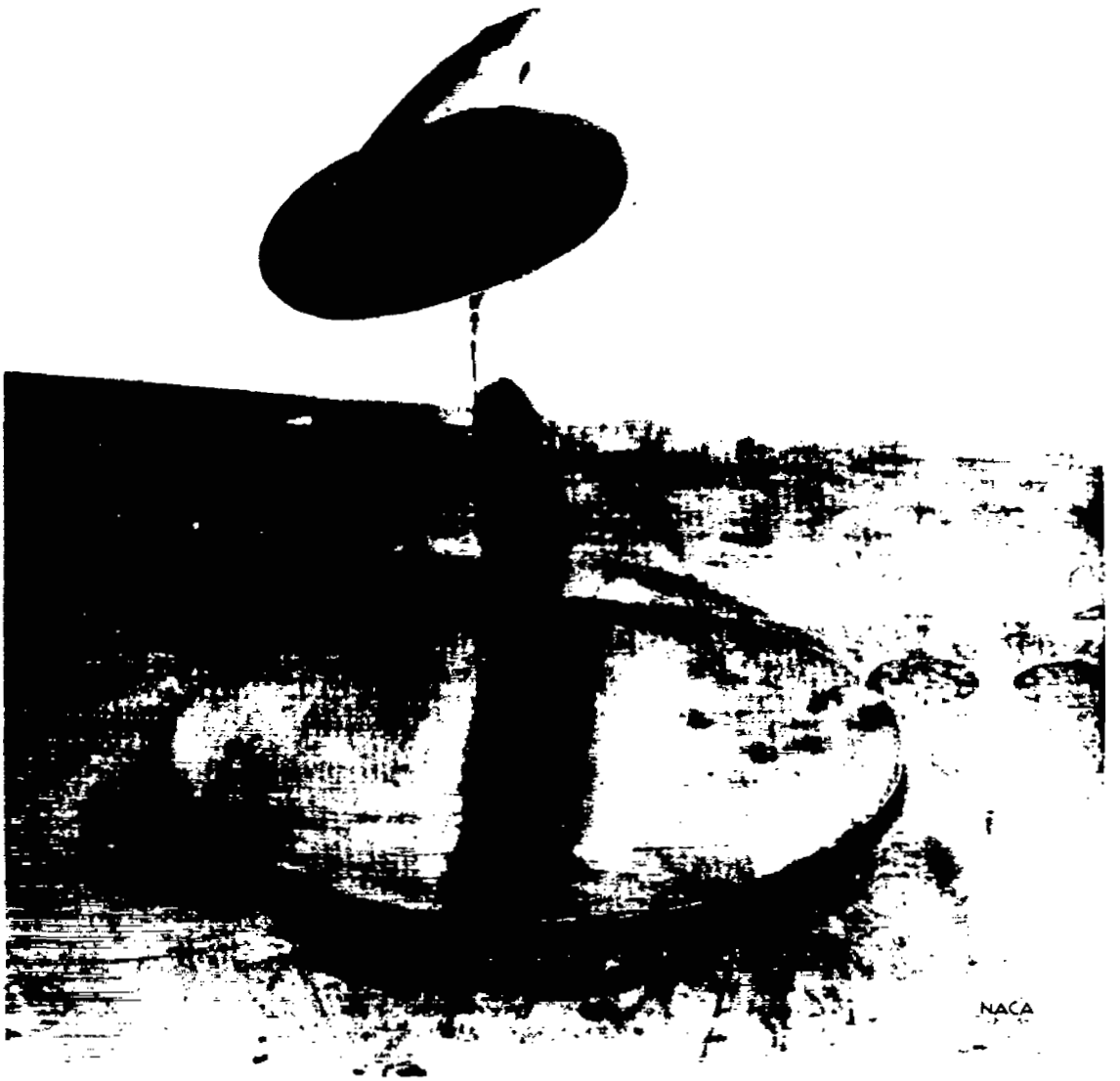

Figure 3.- Model with end plate on root of wing-tip control surface.

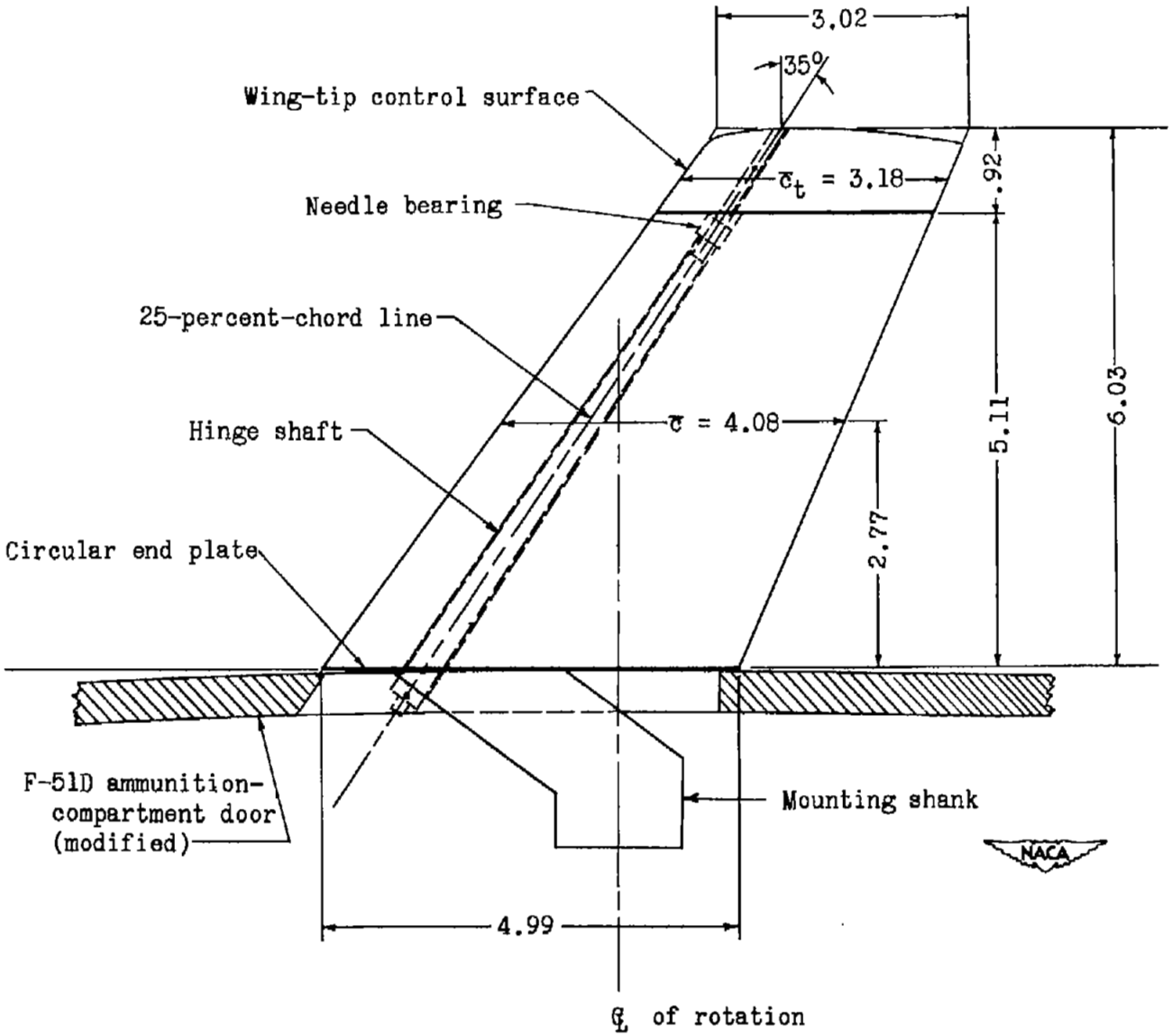

Figure 4.- Drawing of the model.

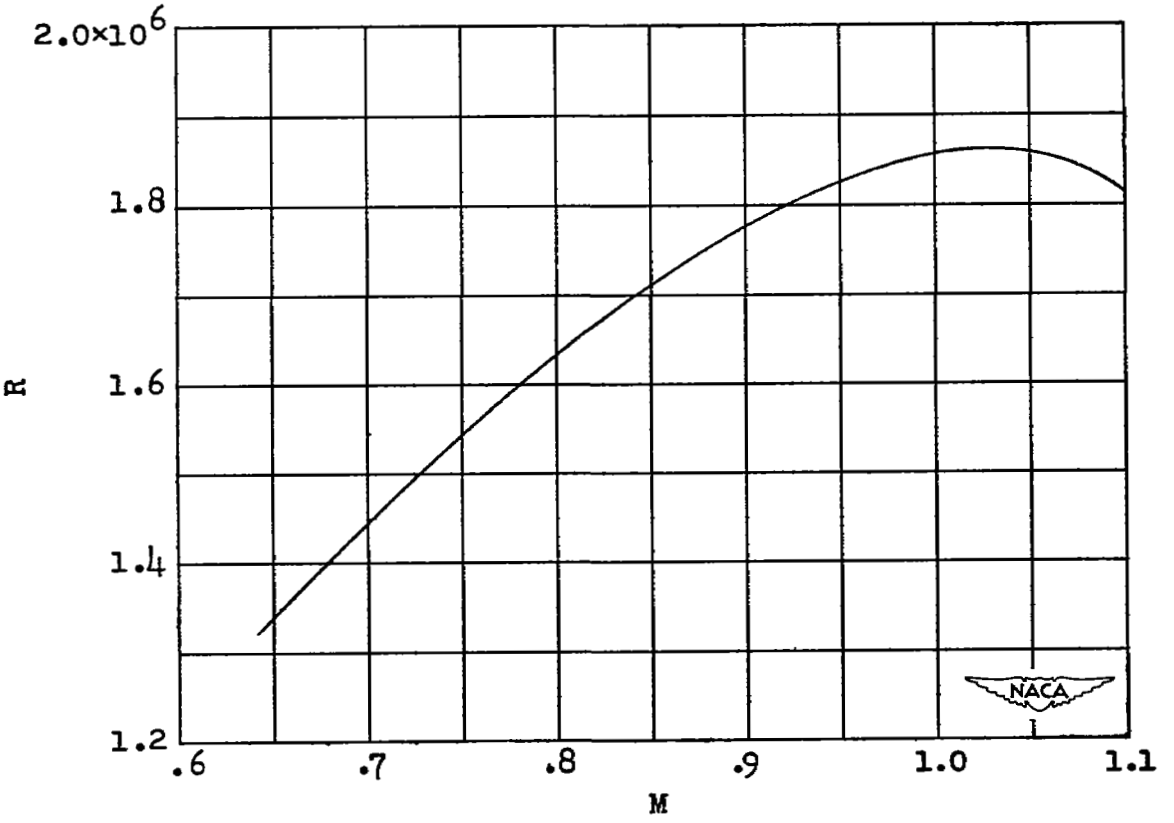

Figure 5.- Variation of Reynolds number with Mach number.

[redacted]

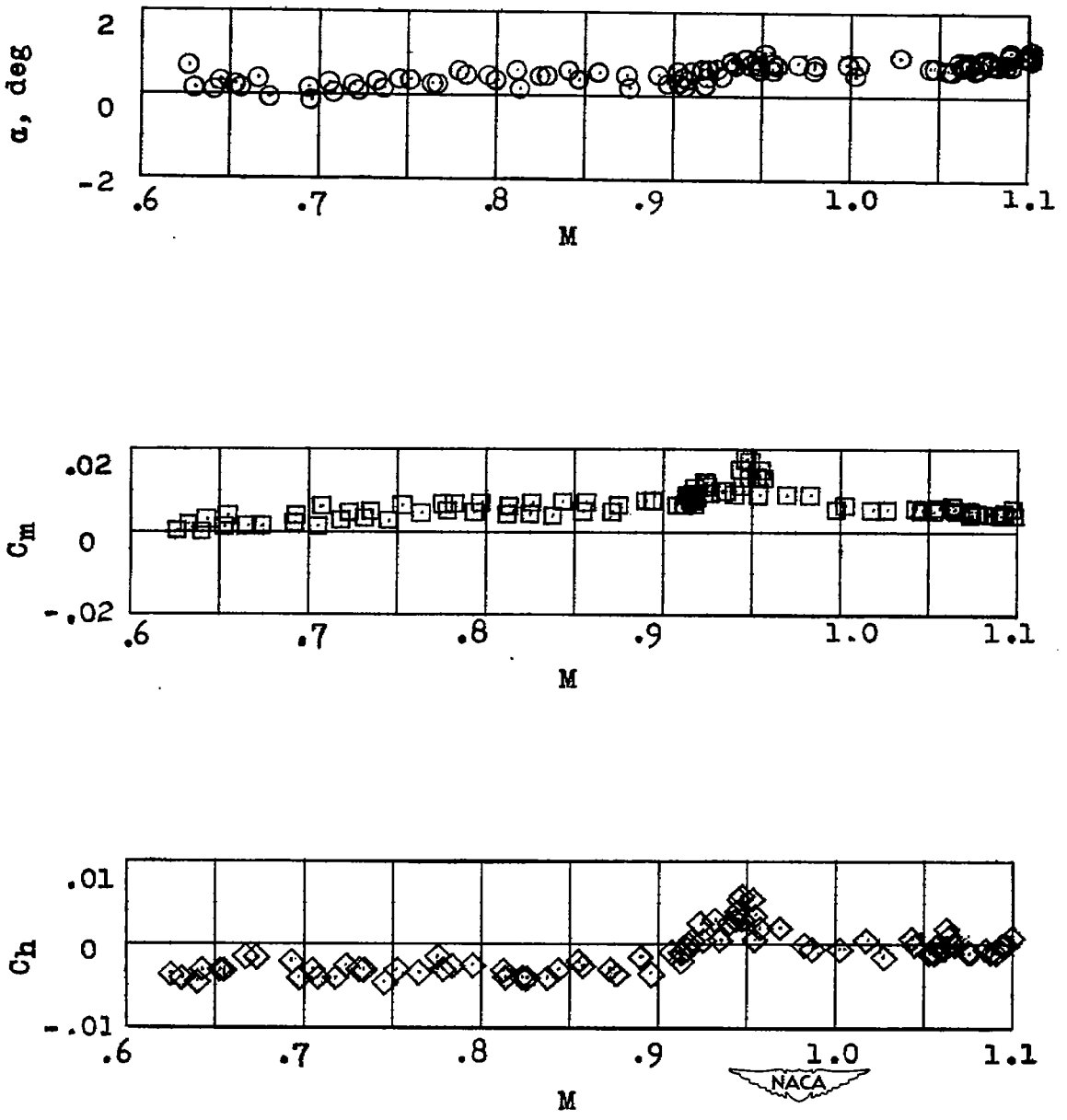

Figure 6.- Typical example of data obtained in wing-flow tests. $\delta = -0.5^{\circ}$; $C_N = 0$.

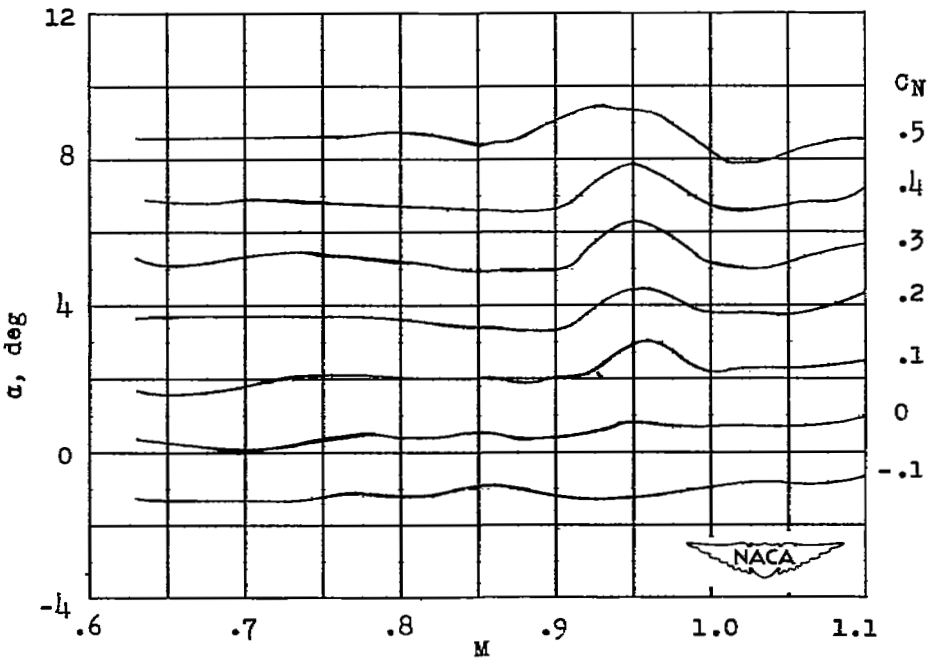

Figure 7.- Variation of angle of attack with Mach number for several normal-force coefficients. $\delta = -0.5^\circ$.

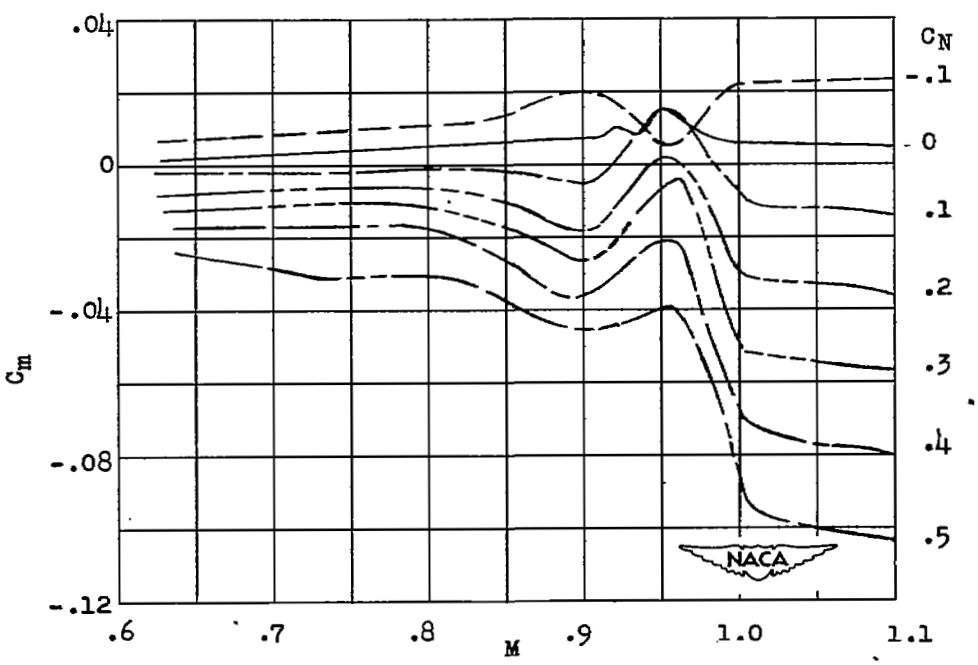

Figure 8.- Variation of pitching-moment coefficient with Mach number for several normal-force coefficients. $\delta = -0.5^\circ$.

[redacted]

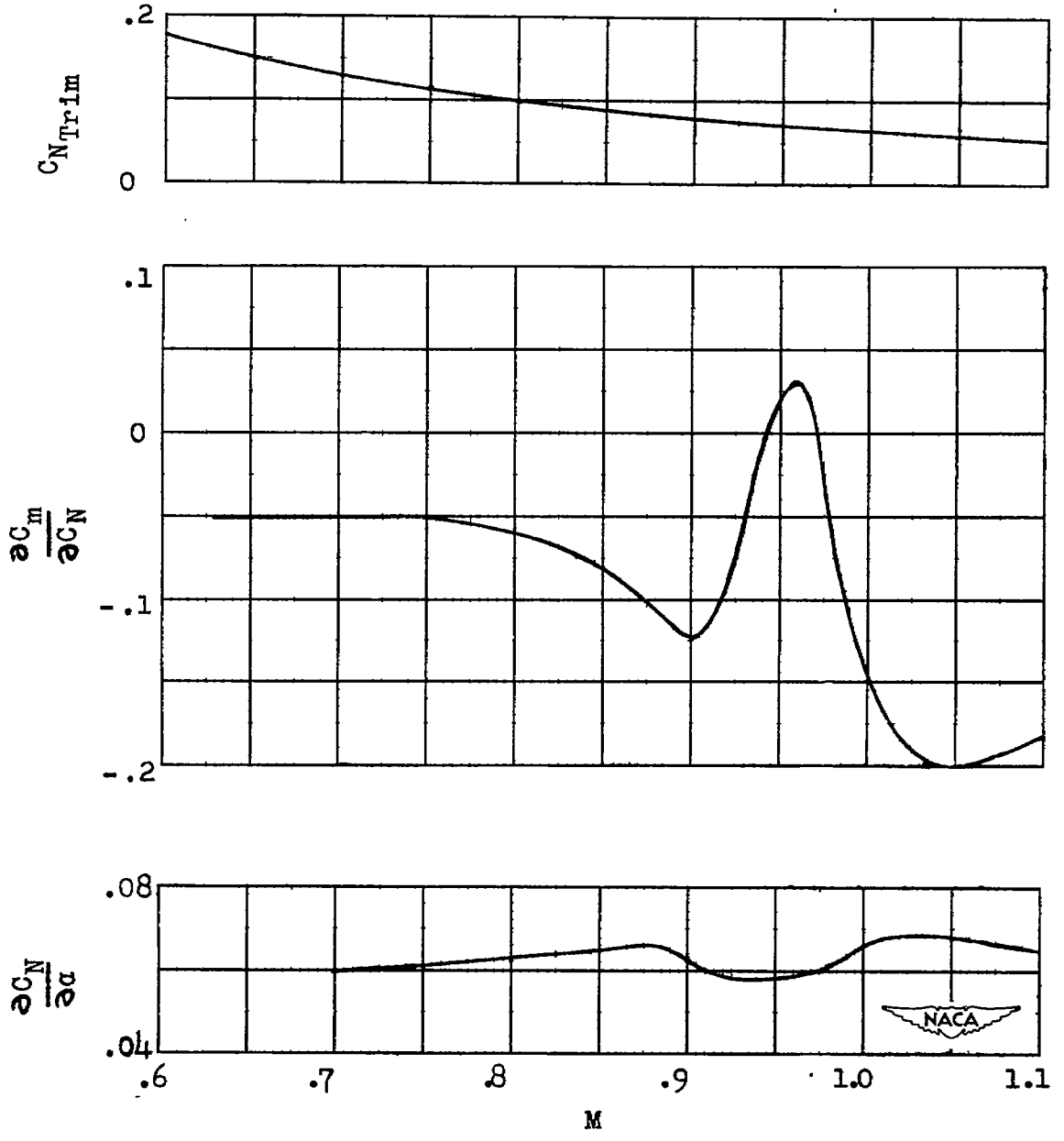

Figure 9.- Variation of normal-force-curve slope and pitching-moment-curve slope with Mach number for wing loading of 28 pounds per square foot, pressure altitude of 30,000 feet, and δ of -0.5°.

[redacted]

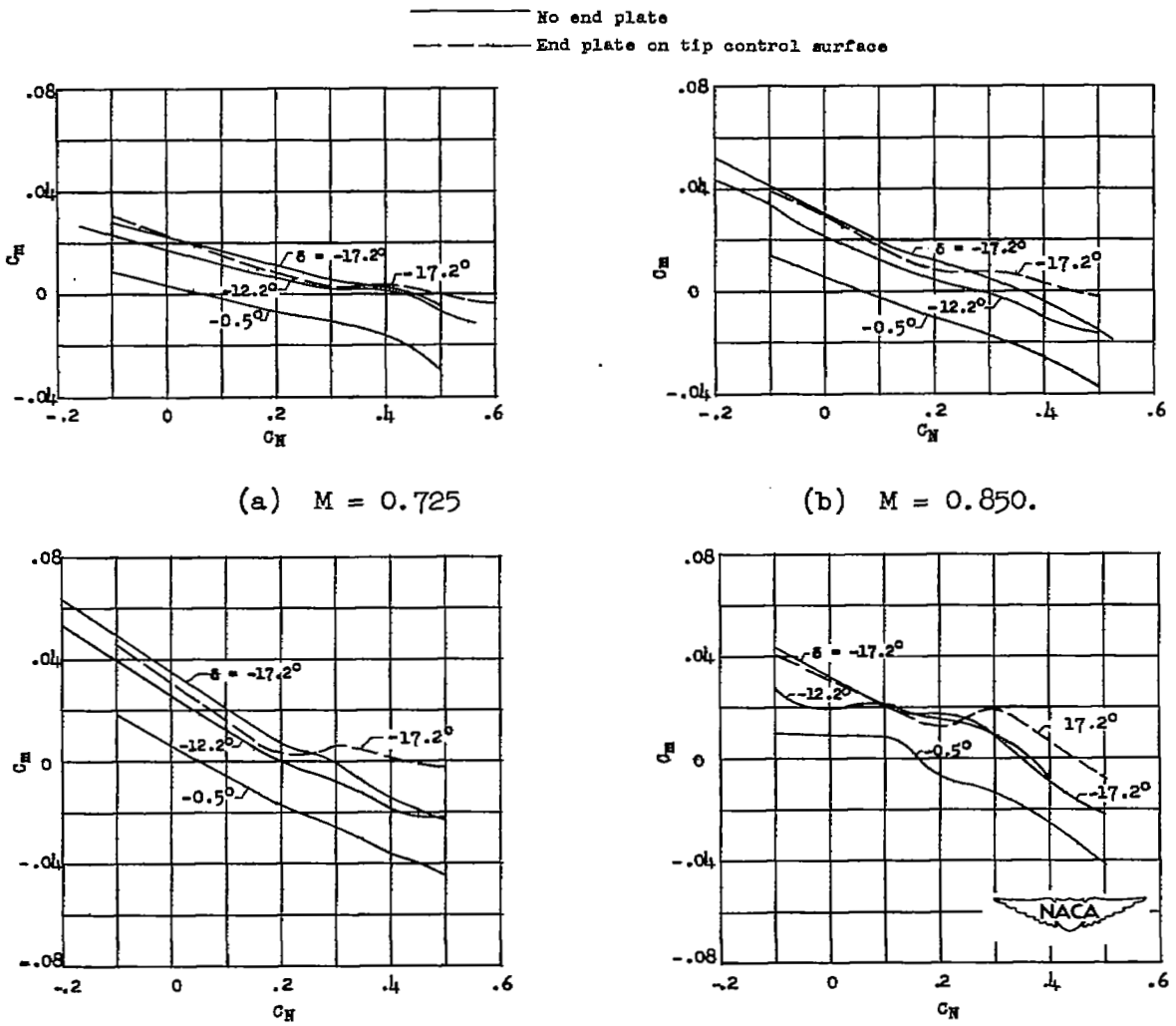

(a) M = 0.725

(b) M = 0.850.

(c) M = 0.890.

(d) M = 0.933.

Figure 10.- The variation of pitching-moment coefficient with normal-force coefficient for several control deflections with and without end plates at various Mach numbers.

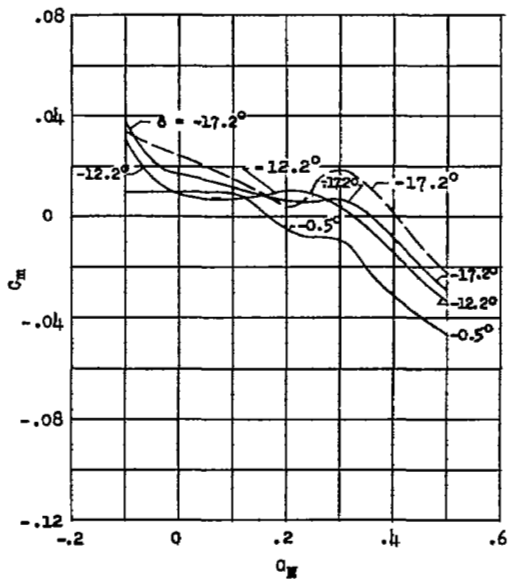

(e) M = 0.970.

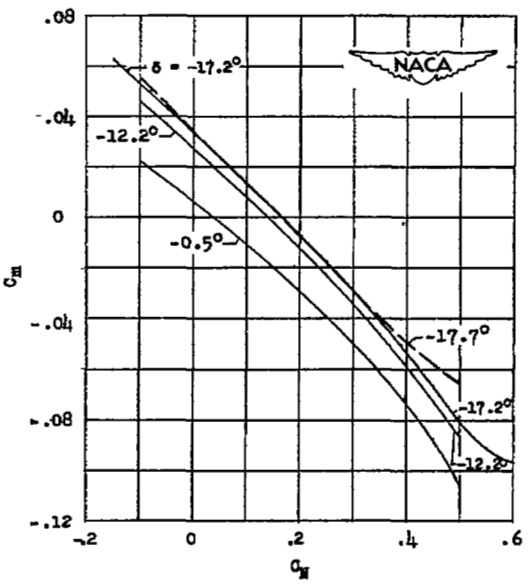

(f) M = 1.01.

Figure 10.- Continued.

[redacted]

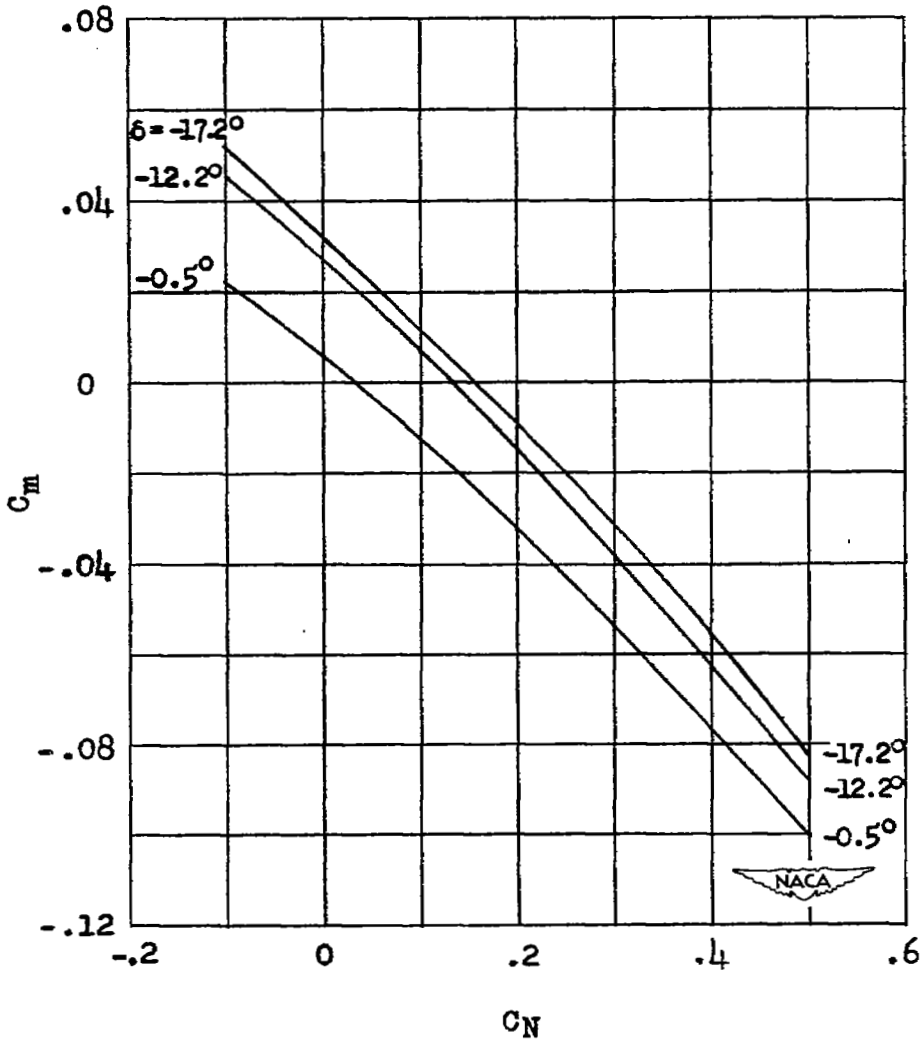

(g) M = 1.05.

Figure 10.- Concluded.

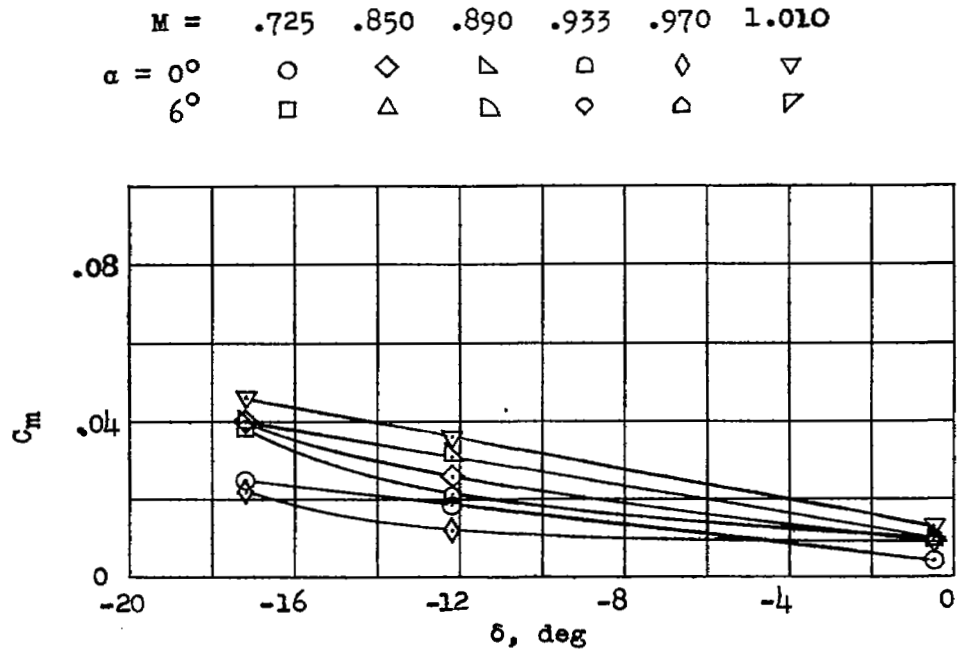

(a) $\alpha = 0^\circ$.

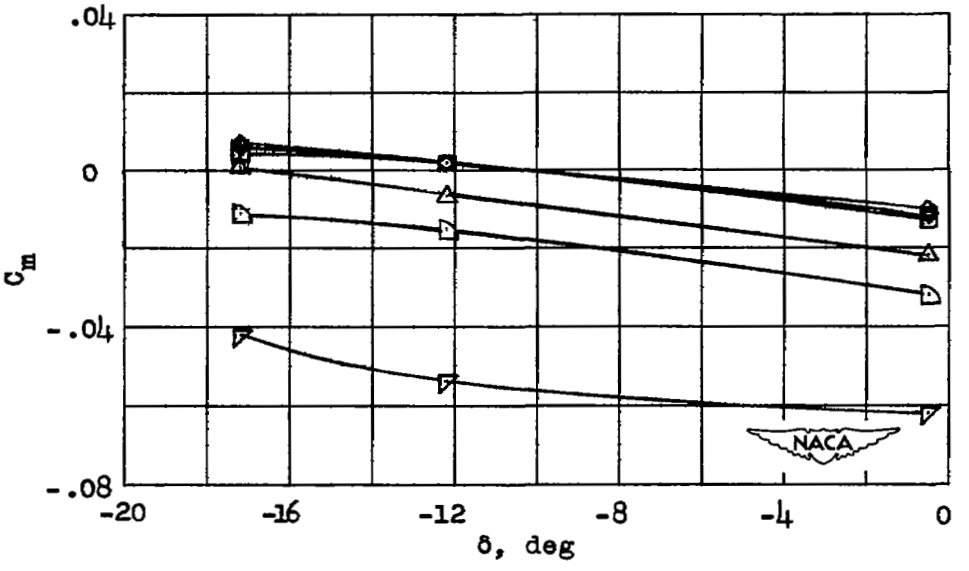

(b) $\alpha = 6^\circ$.

Figure 11.- The variation of pitching-moment coefficient with control deflection for 0° and 6° angles of attack at various Mach numbers.

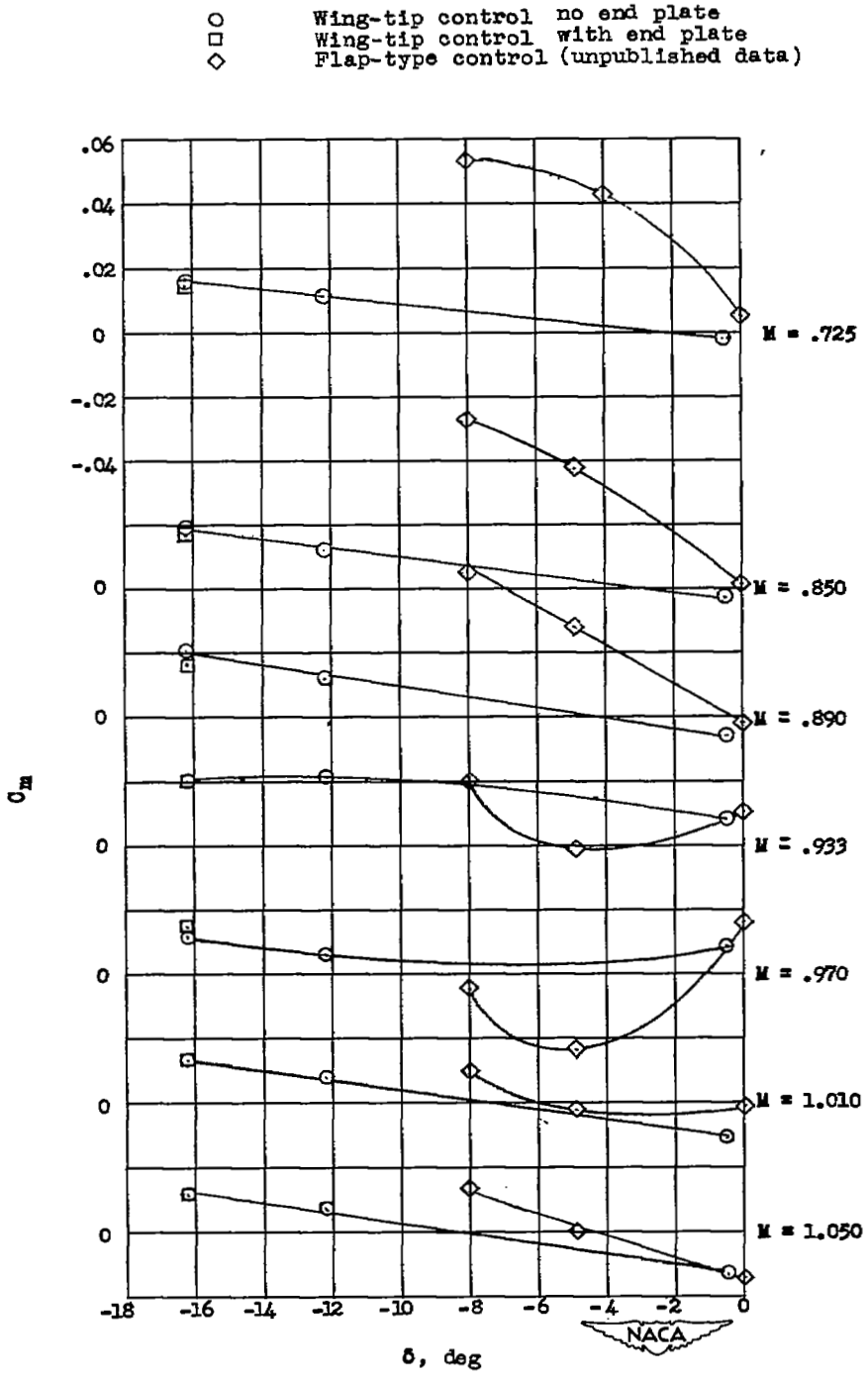

Figure 12.- The variation of pitching-moment coefficient with control deflection for normal-force coefficient of 0.1 at various Mach numbers. Results from fin-off flap-type configuration presented for comparison.

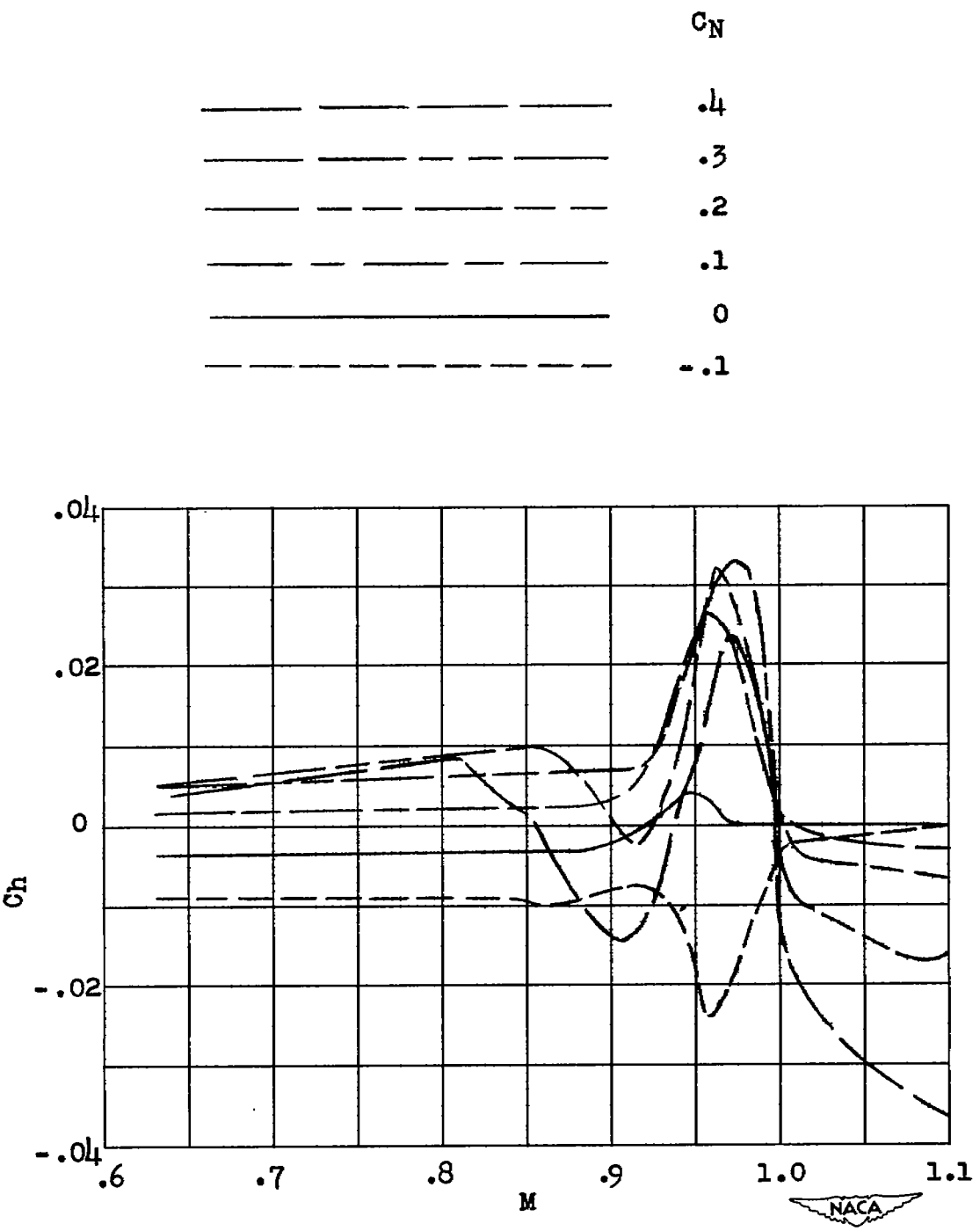

Figure 13.- Variation of hinge-moment coefficient with Mach number for several normal-force coefficients. $\delta = -0.5^\circ$.

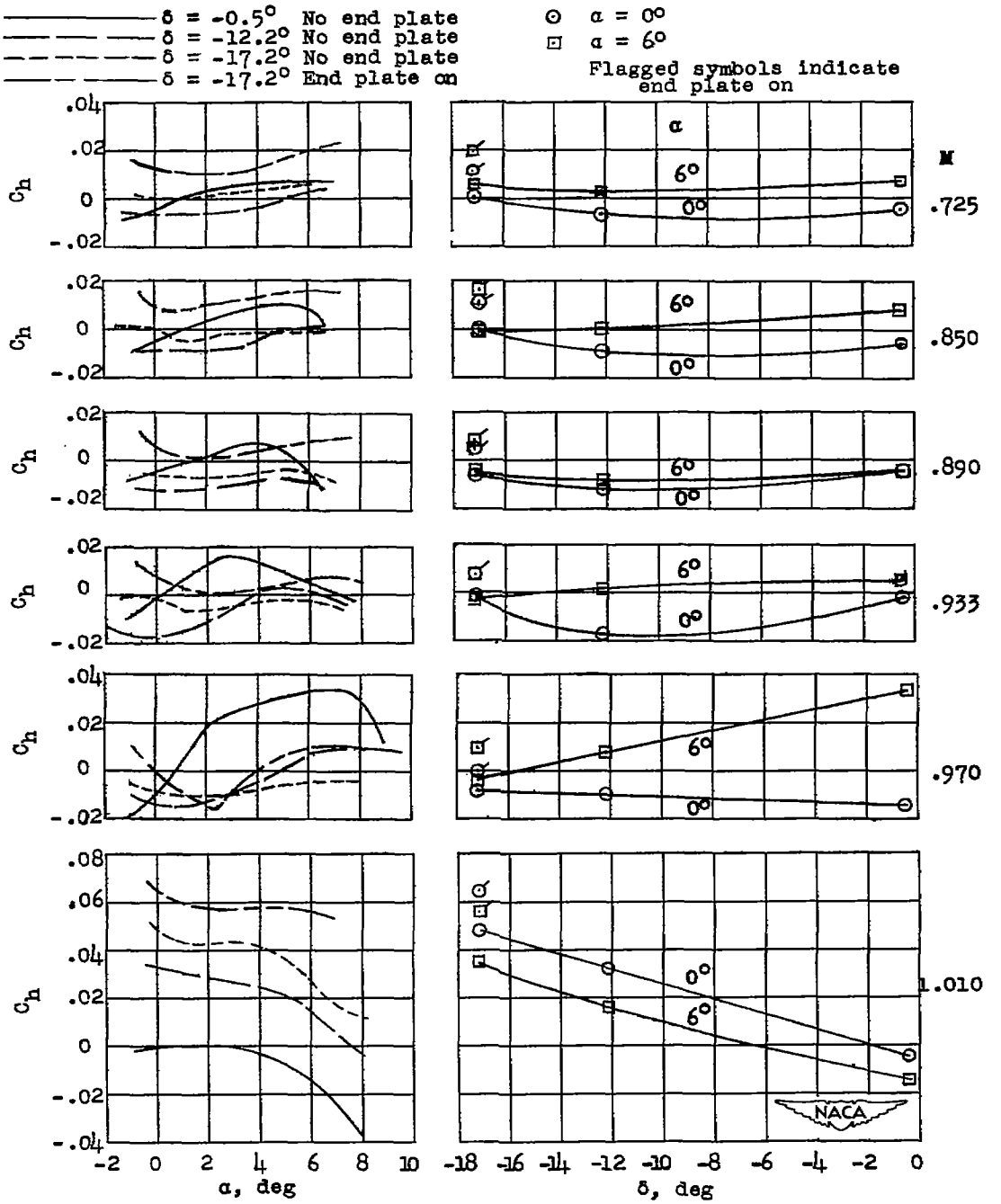

Figure 14.- Variation of hinge-moment coefficient with angle of attack for three control deflections at several Mach numbers.

Figure 15.- Variation of hinge-moment coefficient with control deflection for angles of attack of 0° and 6°.

[redacted]

[redacted]